Tables of Lu et al. [21] show the event time sequence during substorms.

Table S1 Time sequence of various events during the 0736 UT substorm

UT	Spacecraft/instrument	Local time	Descriptions of observational events	Reference
0703	LANL 84/SOPA	20:00	Proton fluxes (50–400 keV) start decreasing	Figure 9
0704	Goes12/M-meter	02:06	Magnetic field lines stretch tailward	Figure 8
0714	Goes10/M-meter	22:04	Magnetic field lines stretch tailward	Figure 8
0722	TC-2/NUADU	Global	Ring current ion fluxes begin increasing	Figure 6
0732	LANL 84/SOPA	20:31	Proton fluxes(50-400 keV) start increasing	Figure 9
0733	LANL 84/MPA	20:33	Convective flows turn Earthward	Figure 9
0735	Goes10/M-meter	22:32	Magnetic field lines show dipolarization	Figure 8
0737	Goes12/M-meter	02:28	Magnetic field lines show dipolarization	Figure 8
0744	TC-2/NUADU	Global	Ring current ion fluxes reach their maximum and start decaying	Figure 6
0800	Ground station		Auroral electrojet, AL-index bay	Figure 7

Table S2 Time sequence of various events during the 0822 UT substorm

UT	Spacecraft /instrument	Local time	Descriptions of observational events	Reference
0803	Goes10/M-meter Goes12/M-meter	23:01 03:03	Magnetic field lines stretch tailward at about the same time	Figure 8
0806	LANL 84/SOPA	21:06	Proton fluxes (50–400 keV) start decreasing	Figure 9
0820	TC-2/NUADU	Global	Ring current ion fluxes begin increasing	Figure 6
0825	Goes10/M-meter	23:36	Magnetic field lines show depolarization [a)]	Figure 8
0826	Goes12/M-meter	03:27	Magnetic field lines show dipolarization	Figure 8
0836	LANL-84/MPA	21:36	Convective flows turn earthward	Figure 9
0840	LANL 84/SOPA	21:29	Proton fluxes (50–400 keV) show a sharp increase (injection signal)	Figure 9
0842	TC-2/NUADU	Global	Ring current ion fluxes reach their maximum and start decaying	Figure 6
0855	Ground station		Auroral electrojet, AL-index bay	Figure 7

a) Since the growing of *Hp* not accompany with *Hn* decreasing at 0818 UT, it was not identified as the dipolarization.

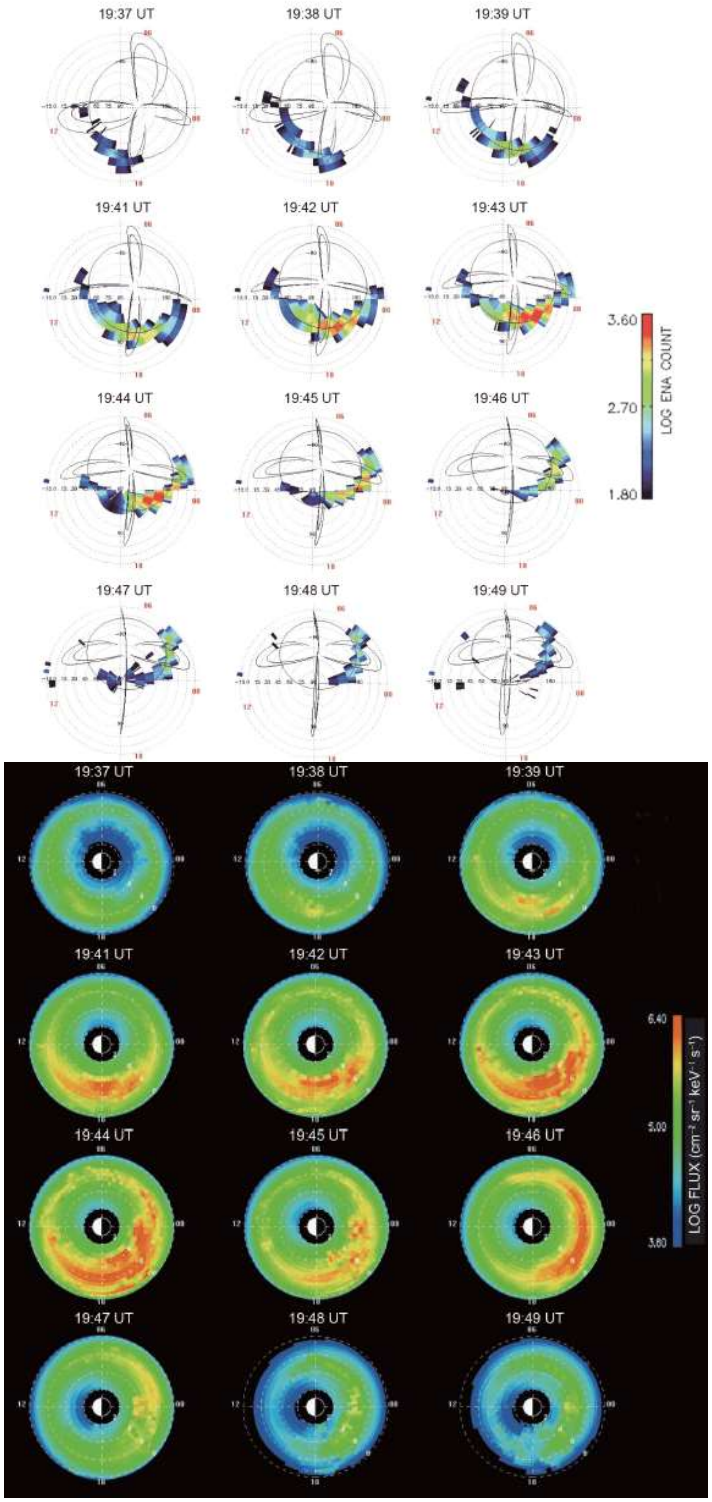

Figure S1. Lu et al.'s [22] evolutionary sequence diagrams show the azimuth drift of the ENA aurora during a substorm.

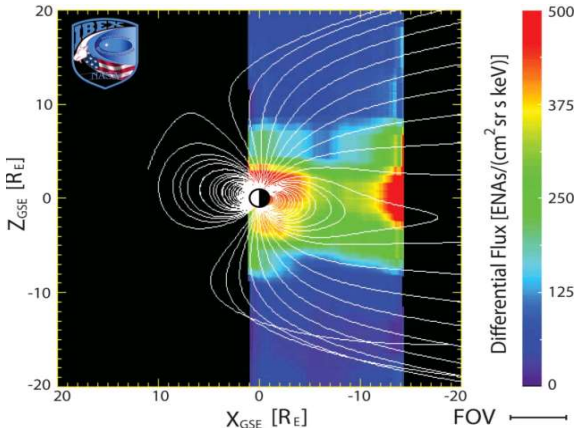

Figure S2. Figure 3 of Mccomas et al. [10]

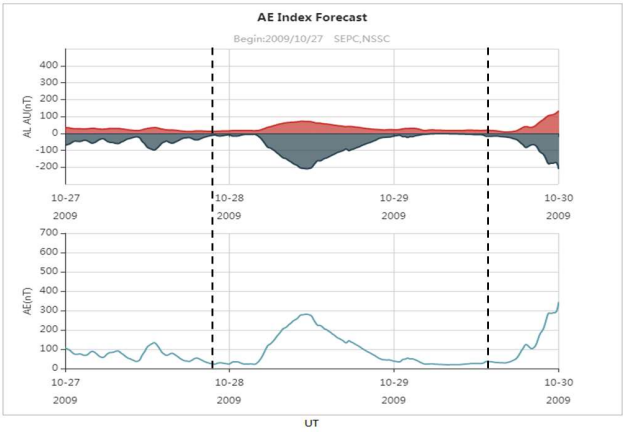

Figure S3. AE index curve of substorm corresponding to magnetotail scanning images of IBEX orbit 51. The region between the two black vertical dotted lines is the sampling period of Figure S2.

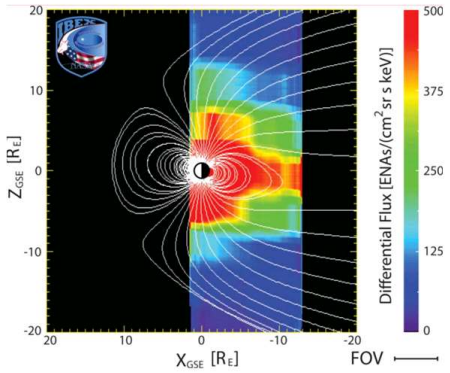

Figure S4. Figure 2 of Mccomas et al. [10]

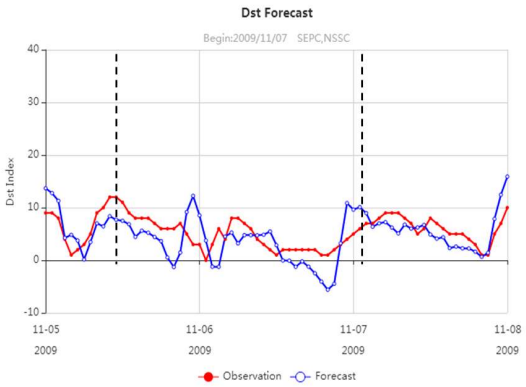

Figure S5. Time-varying curves of Dst index corresponding to ENA scanning images of IBEX orbit 52, where observation in red and forecast in blue (the right panel).

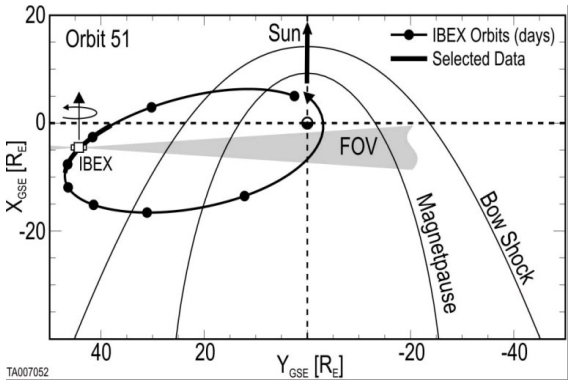

Figure S6. Figure 1 of Mccomas et al. [10] shows orbital positions with periods of 8 days, where the dates are indicated by black dots.

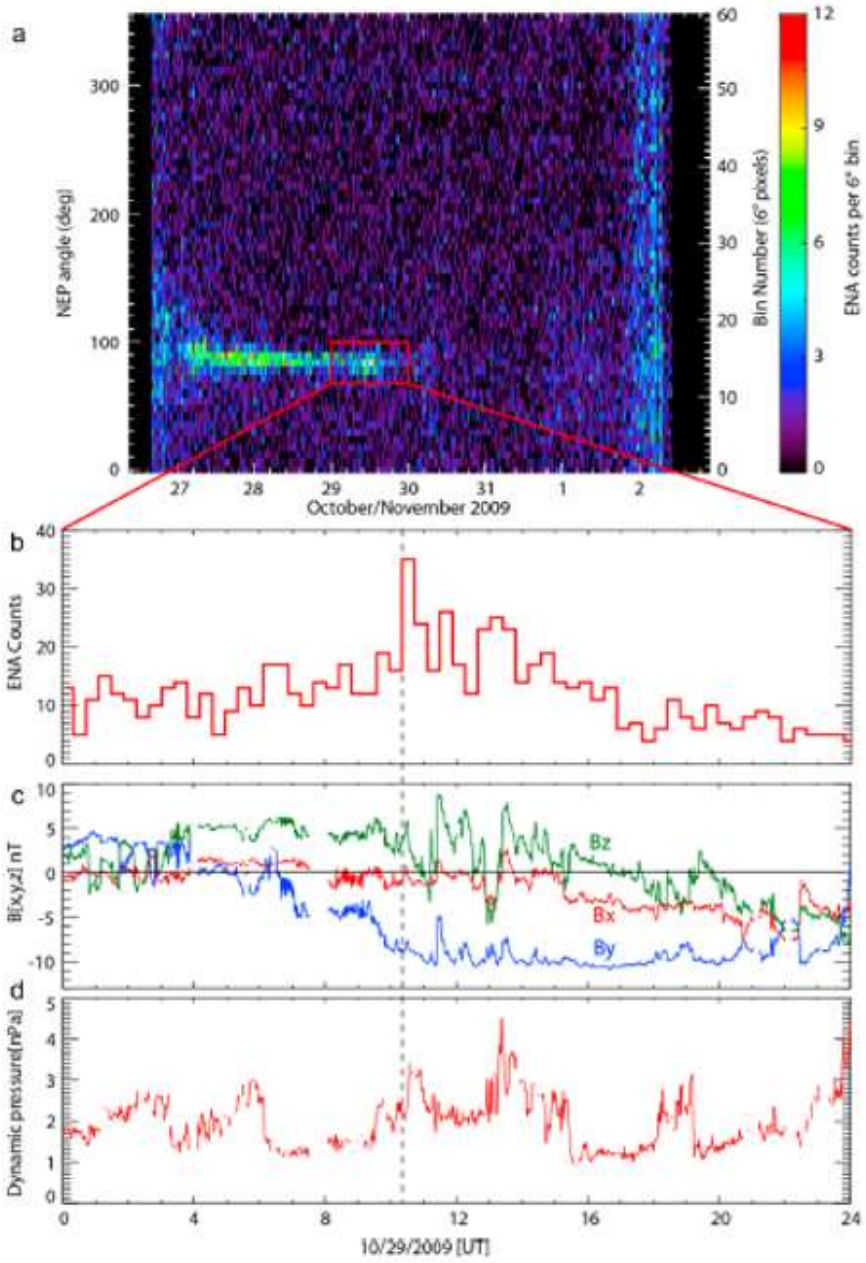

Figure S7. The Figure 4 of McComas et al. [10] shows the raw data. (a) IBEX-Hi energy step 5(2.0-3.8 keCV FWHM) ENA counts for all of IBEX Orbit 51, with the magnetospheric emissions producing the bright band at an NEP angle of ~90°. (b-d) Shown are details from 20 October 2009, when the intensification occurred. Figure 4b gives the integrated counts over 30° inspin phase centered on the magnetotail. Figures 4c and 4d show propagated ACE solar wind parameters for this day.